https://doi.org/10.5194/egusphere-2026-5000
Preprint. Discussion started: 1 September 2026

Detecting soil moisture drought impacts on ecosystem physiology from earth observation data

Yousra El-Mejjaouy[1,2], Koen Hufkens[3], and Benjamin D. Stocker[1,2]

[1]Oeschger Centre for Climate Change Research, University of Bern, Bern, Switzerland,
[2]Institute of Geography, University of Bern, Bern, Switzerland,
[3] BlueGreen Labs (bv), 9120 Melsele, Belgium

Correspondence to: Yousra El-Mejjaouy (yousra.el-mejjaouy@unibe.ch)

Abstract

Satellite remote sensing is widely used to monitor vegetation drought impacts, yet water stress triggers both structural changes and physiological adjustments, whose relative importance varies across space and time. Structural responses, captured by multispectral vegetation indices are well documented, while the extent to which readily available satellite data can detect physiological drought effects remains insufficiently quantified.

Here, we assess how much information on drought-induced physiological responses is contained in multispectral reflectance, land surface temperature (LST), and climate reanalysis data. We combine MODIS reflectance and thermal data with an ERA5-Land potential cumulative water deficits metric (PCWD), and train a machine-learning model using eddy covariance data. The target variable represents drought-induced reductions in light use efficiency (fLUE), explicitly separating physiological regulation from structural canopy changes.

Our resulting data-driven model captures variations in drought-related physiological response more accurately than previously documented indices commonly applied for drought monitoring (R^2 = 0.64, RMSE = 0.112, spatial cross-validation). Application across central Europe during two recent summers demonstrates that the model detects drought impacts on photosynthesis earlier and more sensitively than NDVI, particularly in evergreen ecosystems where structural signals are muted.

Our results show that a systematically trained, data-driven integration of multispectral reflectance, thermal signals, and climate data can extract a substantial portion of the physiological drought response from Earth observation data. This approach enables a more confident and spatially consistent assessment of drought impacts on photosynthesis using the full combined information content of satellite and climate datasets, beyond what structural vegetation indices alone can provide.

https://doi.org/10.5194/egusphere-2026-5000
Preprint. Discussion started: 1 September 2026

1. Introduction

Droughts are important in driving impacts on vegetation, the carbon cycle, agriculture, and water resources. Our understanding of the timing, magnitude and extent of drought impacts on vegetation is crucially informed by satellite remote sensing data. Greenness vegetation indices, such as the Normalized Difference Vegetation Index (NDVI) and the Enhanced Vegetation Index (EVI), the near-infrared reflectance of vegetation (NIR), and the fraction of absorbed photosynthetic active radiation (fAPAR) are widely used for the quantification of drought impacts on terrestrial photosynthesis and on vegetation, the carbon cycle, and agriculture (Reichstein et al. 2013; Zscheischler et al. 2013; Xie and Fan 2021; Chaudhari, Sardar, and Ghosh 2023; Hermann et al. 2023; Chen et al. 2025). These indices are derived from multispectral imaging, available, e.g., from long-term and high resolution satellite missions with global coverage (e.g., MODIS, Landsat, Sentinel-2, AVHRR). Ease of availability and use has spurred research on drought impacts based on data products emerging from such indices.

However, these greenness indices primarily measure structural changes and reflect the amount of active green foliage (Cai et al. 2025; World Meteorol. Organ. 2024), but the mechanistic connection to and quantitative influence by the physiological response of photosynthesis to water stress is often unclear. Short-term and moderate levels of limitation of photosynthesis and transpiration by low root zone water availability or by dry ambient air often have a limited effect on canopy structure and the overall greenness of vegetated land surfaces, but can significantly reduce ecosystem carbon and water vapour fluxes through stomatal closure and other physiological responses that affect the photosynthetic light use efficiency (LUE) (B. D. Stocker et al. 2018a; W. Li et al. 2024). The reduction of stomatal conductance under limited root zone water availability and/or dry air is a key physiological response and affects the diffusion of CO2 inside leaves and its subsequent assimilation through photosynthesis (Lin et al. 2015; Medlyn et al. 2011; Cowan and Farquhar 1977; Oren et al. 1999; J. Flexas et al. 2004). Other important physiological responses to water stress are linked to changes in the capacities for Rubisco carboxylation and electron transport (Zhou et al. 2013), or to light absorption by photoprotective pigments (Demmig-Adams and Adams 1996; Demmig-Adams and Adams III 2006; Jaume Flexas and Medrano 2002; Jahns and Holzwarth 2012; D'Odorico et al. 2021a) and/or dissipation of absorbed light through non-photochemical quenching (Müller et al. 2001; Jaume Flexas and Medrano 2002). Physiological responses may arise before or in the absence of visible structural responses. In contrast to fast-evolving physiological responses, structural changes, including foliage area or live vegetation cover reductions typically occur under more severe water limitation, persistent over longer periods (Meir, Mencuccini, and Dewar 2015; Flack-Prain et al.

https://doi.org/10.5194/egusphere-2026-5000
Preprint. Discussion started: 1 September 2026

2019). It remains challenging to capture the relatively fast physiological response of vegetation, in addition to the structural response, from the analysis of vegetation greenness indices.

To some extent, the physiological response might correlate with the structural response, observable from greenness indices. Indeed, bulk evaluations suggest that greenness indices correlate well with gross primary production (GPP), measured by eddy covariance data from multiple sites, covering multiple years, and reflecting both structural and physiological responses to water stress (John A. Gamon et al. 2016; Badgley et al. 2017; X. Li et al. 2018). However, strong reductions in LUE in response to water stress are also evident (B. D. Stocker et al. 2018a) and suggest that the physiological response may lead - at least partly - to a decoupling between vegetation greenness and ecosystem photosynthesis. From these bulk evaluations, it remains unclear where the limits lie in using greenness indices to assess and quantify vegetation activity and drought impacts on the carbon cycle, and under what specific conditions, such as vegetation types or levels of water stress, the structural and physiological responses deviate.

A range of indices have been proposed to estimate vegetation stress from reflectance bands available from global multispectral missions (Loaiza et al. 2024). However, they generally make *a priori* choices for the consideration of specific bands - usually a subset of all available bands - and functional relationships. Remotely sensed sun-induced fluorescence (SIF) and other sensing modalities, e.g. microwave remote sensing, provide complementary information and have been argued to relate more directly to vegetation's physiological response to water stress (Gu et al. 2023; W. Li et al. 2023; Ying Wang et al. 2024; Qiu et al. 2024). However, these data usually have lower spatial and temporal resolution, limited temporal coverage, and require targeted spectral sensing with relatively narrow bandwidths, which is not supported by readily available global long-term missions such as MODIS, VIIRS, Landsat, or Sentinel-2. Physiological responses are also reflected in changes in chlorophyll and carotenoid content, which can be detected using multispectral reflectance data and derived indices, including PRI (J. A. Gamon et al. 1992; Garbulsky et al. 2011; D'Odorico et al. 2021b). However, an application of these methods across larger scales and across diverse land cover types and ecosystems remains challenging. Yet, alternative spectral reflectance indices and thermal remote sensing measure different canopy and leaf properties that relate to photosynthesis and water stress. They bear complementary information to common greenness indices, indicating that key information relevant for water stress detection and quantification is contained in multispectral reflectance and thermal remote sensing data, but is not fully exploited by commonly used vegetation indices for drought impact studies.

The limited link of remote sensing data with the physiological response of plants to water stress is also due to an observational challenge. Eddy covariance measurements of ecosystem-atmosphere exchange

https://doi.org/10.5194/egusphere-2026-5000
Preprint. Discussion started: 1 September 2026

fluxes are a mainstay for calibrating and "groundtruthing" remote sensing data for interpretations related to ecosystem functioning, CO_2 fluxes, and photosynthesis (Yin et al. 2022; B. D. Stocker et al. 2018a; Middleton et al. 2016). However, these data measure the combined effect of the structural and physiological responses to water stress, and it is challenging to interpret the physiological component directly (Yanbing Wang et al. 2023; W. Li et al. 2024). Instead, observations of the physiological response are commonly obtained through leaf-level measurements of, e.g., stomatal conductance, or photosynthetic capacities. Because these measurements are laborious, the volume of related data is limited and thus cannot easily be used in connection with continuous global-scale remote sensing.

One solution to this challenge was recently developed by Stocker et al. (2018). These authors assessed drought-induced physiological stress from eddy covariance flux measurements and soil moisture data. Their artificial neural network framework was used to separate reductions in photosynthetic efficiency caused by soil moisture limitation from concurrent changes in vegetation greenness. Thus, they developed a metric to quantify the fractional reduction in light use efficiency (fLUE) due to soil moisture stress. Light use efficiency was defined at the ecosystem-level as the ratio of GPP over absorbed photosynthetically active radiation. This approach allowed for the estimation of soil moisture-mediated physiological response, isolated from the structural response, and was applied across a broad range of vegetation types and climatic conditions. Building on this framework, we use independently derived fLUE estimates as a physiological target and test whether they can be predicted spatially from MODIS multispectral reflectance and thermal infrared observations, enabling large-scale monitoring of drought-induced physiological responses separately from structural vegetation changes.

Here, we exploit this potential and use fLUE as a starting point. We use a machine learning method to develop a generally applicable EO-based model for the quantification of the physiological response of ecosystem photosynthesis to water stress. To address this, we used estimates of the magnitude of soil moisture drought stress on light use efficiency (fLUE) from globally distributed sites, provided by Stocker et al. (2018), as a target for a data-driven model that uses the full spectral reflectance signal and the thermal band from MODIS, combined with climate data. Thus, we investigated the extent to which the physiological drought response can be sensed from readily available remote sensing data with long-term (>20 years) global coverage. To evaluate the effectiveness of our satellite-derived index ($fLUE^*$) in capturing physiological impacts of soil moisture drought and in generalising across different ecosystem types, we compared its response with that of the normalised difference vegetation index (NDVI) and a set of other vegetation indices that have previously been used for remote sensing-based drought monitoring. The comparison of $fLUE^*$ and NDVI is then extended to assessing their spatial patterns across central Europe during the severe 2018 drought (Kowalski et al. 2022), compared to the more moist summer conditions in 2020.

https://doi.org/10.5194/egusphere-2026-5000
Preprint. Discussion started: 1 September 2026

2. Methods

2.1. Study sites and target data

We obtained data from 69 sites, covering 644 site-years, for which the target variable of our analysis and models, fLUE, was provided (B. D. Stocker et al. 2018a; B. Stocker 2018). The study sites are globally distributed and cover five vegetation classes comprising, evergreen needleleaf forest (ENF), grassland (GRA), savanna and woody savanna (SAV), evergreen broadleaf forest (EBF), and deciduous broadleaf forest (DBF) (Fig. 1). The sites are grouped into four clusters based on their vegetation responses to soil moisture drought with cDD referring to the drought-deciduous cluster of sites, cGR to the evergreen cluster, and cLS to the cluster of sites where vegetation appears to have a low sensitivity to low root zone moisture. At sites in cNA, LUE was not affected by low soil moisture (Stocker et al. 2018). These sites were originally selected by (B. D. Stocker et al. 2018a) from 166 sites provided through the FLUXNET2015 dataset (Pastorello et al. 2020). Their selection was based on the availability of good-quality data, covering at least 500 days per site, and the performance of their site-specific models in predicting LUE variations. fLUE measures a soil moisture drought magnitude, estimated as the ratio of actual to potential LUE. Their models predicted LUE using a machine learning approach, trained on observed FLUXNET data and environmental drivers including air temperature, photosynthetically active radiation (PAR), vapour pressure deficit (VPD), and soil moisture. They derived LUE by dividing GPP, estimated from eddy covariance measurements and the nighttime flux partitioning method, by the product of PAR and fAPAR, where fAPAR was obtained from MODIS EVI (MOD13Q1, Collection 5) and, alternatively, from MODIS FPAR (MOD15A2). The separation of the physiological and structural response of photosynthesis to root zone water stress was thus achieved by assuming that EVI (FPAR) fully and exclusively capture the structural response.

https://doi.org/10.5194/egusphere-2026-5000
Preprint. Discussion started: 1 September 2026

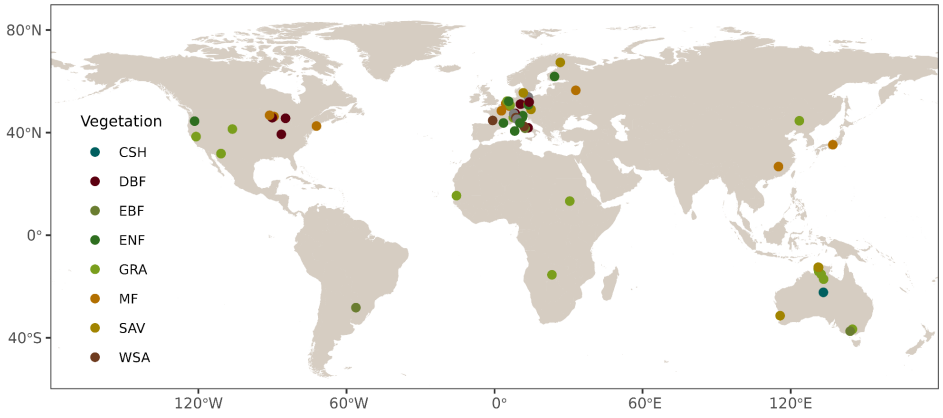

Fig. 1. Map of the sites used in the analysis, colour-coded by the vegetation class (GRA, grasslands; SAV, savannah; WSA, woody savannah; ENF, evergreen needleleaved forest; EBF, evergreen broadleaved forest; DBF, deciduous broadleaved forest; CSH, closed shrubland; MF, mixed forest).

2.2. Predictor data

We used MODIS reflectance bands, land surface temperature (LST), meteorological drivers from ERA5-Land climate reanalysis, potential cumulative water deficit, normalized differences of all reflectance band combinations, and land cover type as predictors for modelling fLUE (Tab. 1), obtained for the 69 sites described above (Fig. 1). To obtain nadir reflectance and land surface temperature data for single pixels containing the flux tower locations, we created a base query containing site names, latitudes, longitudes, and relevant time frames for each site, submitted to *AppEEARS* (https://appeears.earthdatacloud.nasa.gov/) (Hufkens 2023). Multispectral reflectance data (Tab. 1) was taken from the MODIS MCD43A4 Bidirectional Reflectance Distribution Function (BRDF) adjusted product Version 6.1. Land surface temperature data was taken from the MODIS MOD11A1 product. The MCD43A4 data have a spatial resolution of 500 m and daily temporal resolution, while MOD11A1 provides data with a daily Land Surface Temperature Emissivity with spatial resolution of 1 km.

Poor-quality data were implicitly excluded through the internal quality screening applied in the MODIS products, and additional filtering based upon good data quality using data QA/QC descriptions was performed. The screened bad values were cleaned up and marked as NA. This resulted in a loss of 35-39% for reflectance bands 1, 3, 5, and 7, 3-4% for reflectance bands 2, 4, and 6, and 65% for LST. Prior to model training, we imputed missing data using additional meteorological predictors, extracted from eddy-covariance site records using FluxDataKit (Hufkens and Stocker 2024). For each site and date, daytime mean air temperature (TA_F_MDS) and incoming shortwave

https://doi.org/10.5194/egusphere-2026-5000
Preprint. Discussion started: 1 September 2026

radiation (SW_IN_F_MDS) were added to the dataset. Missing remote-sensing variables were then filled using sequential *k*-nearest-neighbour (KNN) imputation. In the first step, reflectance bands 1, 3, 5, and 7 - those with the highest proportion of missing values - were imputed using air temperature, shortwave radiation, and the remaining reflectance bands 2, 4, and 6 as predictors. In the second step, land surface temperature (LST) was imputed using all reflectance bands together with the same meteorological predictors. Bands 2, 4, and 6 were not imputed. Variables were imputed iteratively using a custom imputation function that trains a KNN model for the target variable and replaces missing values with predicted estimates. The KNN model was specified using normalised values of all predictors and the optimal *k* was selected among (5, 15, 25) based on 5-fold cross-validation. Imputation was done once prior to model training and not implemented as part of the model cross-validation workflow due to prohibitive computational costs and in view of the fact that the target variable of the final model (fLUE) was not used as predictor for any of the imputation steps - thus largely averting the risk of data leakage.

To provide predictors for downstream modelling, additional variables from earth observation and climate data products were merged with the dataset, and other locally measured variables, used for imputation, were dropped again. We used, meteorological data from ERA5-Land, including air temperature at 2 m (t2m_era5), surface solar radiation downwards (ssrd_era5), and the ERA5-Land data-derived potential cumulative water deficit (PCWD, see below), all originally provided at 0.1° spatial resolution. For both ERA5-Land variables and PCWD, the nearest 0.1° grid-cell values to each FLUXNET site of the 69 sites were extracted and added to the training dataset. This resulting dataset, containing fLUE data, spectral reflectance, land surface temperature, and ERA5-Land variables and PCWD for all 69 sites and available dates was used to train the machine learning model.

Potential cumulative water deficit (PCWD) was calculated as the cumulative difference between potential evapotranspiration (PET) and precipitation (P) over continuously dry periods when atmospheric evaporative demand exceeds water supply (B. D. Stocker et al. 2023), following the workflow established by (Helpap et al. 2026). PET was used instead of actual evapotranspiration to isolate atmospheric forcing and avoid uncertainties associated with vegetation processes and model-specific assumptions about soil water storage (Stocker et al. 2024). PET was computed using the Priestley–Taylor equation as implemented by (Davis et al. 2017), which expresses PET as a function of temperature and net radiation. For ERA5-Land, PET was recalculated from daily temperature and monthly net radiation, the latter calculated from surface net solar and thermal radiation (ssr + str). Precipitation was partitioned into rainfall and snowfall using an ERA5-specific snow-simulation scheme that models snow accumulation, melt, and meltwater release; meltwater was added to rainfall to obtain daily liquid water input to the soil (P_{in}). PCWD accumulation begins on the first day when PET exceeds P_{in} and continues until the deficit is compensated, with an absolute

https://doi.org/10.5194/egusphere-2026-5000
Preprint. Discussion started: 1 September 2026

threshold of 10 mm marking the end of a PCWD event. All computations were performed for each ERA5-Land grid cell using the *cwd* R package (Stocker et al. 2024).

Table 1. MODIS spectral bands and ERA-Land variables with their annotations, spectral ranges, and descriptions (Schaaf and Wang 2021; Wan et al. 2021; Muñoz-Sabater et al. 2021)

Product	Short name	Spectral range [nm]	Description
MCD43A4.061	NR_B1	620 - 670	Red
	NR_B2	841 - 876	NIR
	NR_B3	459 - 479	Blue
	NR_B4	545 - 565	Green
	NR_B5	1230 - 1250	SWIR1
	NR_B6	1628 - 1652	SWIR2
	NR_B7	2105 - 2155	SWIR3
MOD11A1.061	LST	-	Land surface temperature
MCD12Q1	LC	-	Land cover
ERA5-Land	t2m_era5	-	2 m air temperature
	ssrd_era5	-	Surface solar radiation downwards
	pcwd_era5	-	Potential cumulative water deficit (derived)

2.3. Modelling

We trained the model that uses data measuring the fractional reduction of light use efficiency due to soil moisture stress (fLUE (B. D. Stocker et al. 2018b)) as the target and seven spectral reflectances (Tab. 1), land surface temperature, and meteorological data (*t2m, ssrd, and pcwd*) as the predictors. The model was implemented as a Random Forest (RF) model, using the *ranger* R package (Wright et al. 2024). Model training was conducted through leave-one-site-out cross-validation to ensure spatial generalization. This approach places data for a specific site either entirely in the training, or entirely in

https://doi.org/10.5194/egusphere-2026-5000
Preprint. Discussion started: 1 September 2026

the validation set and yields models that should be generalisable across sites. We performed the following pre-processing steps as part of the cross-validation workflow. First, all possible pairwise combinations of MODIS surface reflectance bands were computed as normalized difference indices (nd_NR_BX1_NR_BX2) and incorporated as predictors in the model. Second, all numeric predictors were normalised. Third, the predictor *vegetation type* was dummy-encoded. Fourth, data points belonging to periods with substantial fLUE reductions ('fLUE droughts' as defined in the data by (B. Stocker 2018)) were up-sampled to have the same ratio as non-'fLUE droughts'. Hyperparameters were tuned using a grid search over *mtry* (3, 5, 7) and minimum node size (min.node.size) (5, 15, 25), while the split rule was fixed to *variance*. Hyperparameters were optimized with *mtry* = 7, *min.node.size* = 15, and 500 trees. Training used bootstrap sampling (fraction = 0.5) and 500 trees, and the final model was refitted with 2,000 trees for improved stability. Variable importance analysis based on impurity reduction identified the most influential predictors for predicting the physiological drought impacts on vegetation.

2.4. Comparison of fLUE* with common spectral vegetation indices

2.4.1. Linear correlation between fLUE* and vegetation indices

We compared the correlation between fLUE and fLUE* (predicted value of fLUE) with the correlation between fLUE and a set of commonly used vegetation indices (VIs) to understand how well remote sensing-based indices capture variations in the physiological response of ecosystem photosynthesis to water stress, as measured by fLUE. For this, we selected the most commonly used vegetation indices for monitoring vegetation drought (Table S1) from a list of spectral indices widely used in remote sensing (Loaiza et al. 2024). The VIs are computed using MODIS nadir reflectance bands (Table. 1) for each date for which fLUE was available. Within each cluster, during 10 days pre-drought onset and drought events (30 days after drought onset), a linear model of fLUE with fLUE* and with the calculated VIs was fitted separately. Then, the R^2 value for each linear model was extracted and plotted to compare the relationship between vegetation indices, fLUE*, and fLUE, and to determine which remote sensing indices best capture the physiological changes in vegetation due to soil moisture drought. The normalised difference vegetation index (NDVI), besides fLUE*, turned out to yield the highest correlation with fLUE (Fig. 3) and was therefore used for subsequent analysis steps, described below. The drought events were defined according to Stocker et al. (2018) as days when fLUE falls below a site-specific threshold. We considered only data from dates that belonged to soil moisture drought events of at least twenty-seven consecutive days. For each site, data from each event was aligned with respect to the first day of the respective event.

https://doi.org/10.5194/egusphere-2026-5000
Preprint. Discussion started: 1 September 2026

2.4.2. Spatial analysis for summers of 2018 and 2020 in central Europe

Using geospatial images (rasters) of multispectral reflectances and LST, we applied the fitted model to predict fLUE* over Central Europe for two contrasting summer conditions, comparing the severe drought of 2018 with more humid conditions in 2020 (Kowalski et al. 2022). For comparison, we calculated NDVI from the same data (Table. S1). Multispectral reflectance and LST data were obtained from the same products as used for training the model (Table. 1). For the LST band, before averaging, the rasters, originally provided at 1 km resolution, were resampled using bilinear interpolation to a spatial resolution of 500 m to be compatible with the resolution of the reflectance rasters. Similarly, the t2m_era5, ssrd_era5, and pcwd_era5 datasets for the Central Europe extent were extracted. Their spatial extents were matched to the MODIS rasters and disaggregated by replication to achieve the same spatial resolution as MODIS for spatial upscaling of the model.

Data for June, July, and August of 2018 and 2020 were obtained and averaged per month and year. The average values for these months were calculated for each band and combined into a raster stack for each year. Pixels covered by croplands, permanent snow, and water bodies, as well as other vegetation types (closed shrublands, deciduous needleleaf forests, open shrublands, and barren or sparsely vegetated areas), represented by a small number of pixels in the study area, were masked. Wetlands were also dropped because of their distinct water-vegetation relations which we did not expect to capture with a single generalised model, informed almost exclusively by data from non-wetland sites. The mask was created using the land cover (LC) product (MCD12Q1) from MODIS and applied to the fLUE* and NDVI rasters. Temporal changes in fLUE* and NDVI during the summers of 2018 and 2020, referred to as ΔfLUE* and ΔNDVI, were analysed as the differences in their values between June and July, and between June and August. Then, the difference between NDVI and fLUE* temporal changes were calculated to compare spatial patterns of temporal changes between both summers. We conducted further analysis of the distribution of the difference between the values of two rasters for the summers of 2018 and 2020. Furthermore, we analyzed ΔfLUE* and ΔNDVI during both summers separately for each vegetation type as the respective mean across pixels covered by the respective vegetation.

To identify areas where these spatial predictions represented interpolation rather than extrapolation, the model's Area of Applicability (AOA) was assessed using the CAST package (Meyer et al. 2026). Euclidean distances in the processed predictor space were weighted by variable importance derived from the final random-forest model. For each prediction pixel, the Dissimilarity Index (DI) was calculated from its distance to the most similar training observation, normalized by the mean nearest-neighbour distance among the training observations. The DI threshold was derived using the same leave-site-out cross-validation folds employed for model evaluation. Pixels with DI ≤ 0.195 were

https://doi.org/10.5194/egusphere-2026-5000
Preprint. Discussion started: 1 September 2026

293 classified as inside the AOA, whereas those with DI > 0.195 were considered extrapolations. Pixels
294 with missing predictor values were excluded.

295 3. Results

296 3.1. fLUE prediction models

297 Fig. 2 presents fLUE out-of-sample prediction performance using MODIS spectral and thermal bands,
298 ERA5-Land variables t2m and ssrd, and potential cumulative water deficit (Fig. 2a). Prediction
299 performances are quantified on pooled data from individual held-out sites of each cross-validation
300 fold. The model predicted fLUE with an R^2 of 0.64 and a RMSE of 0.112 (unitless). The variable
301 importance plot showed that a normalized vegetation index derived from nadir reflectance bands
302 corresponding to red and green (nd_NR_B1_NR_B4) was the most important predictor for fLUE. This
303 index corresponds to the negative of the broadband green-red vegetation index (GRVI). The
304 importance of this index was followed by PCWD and LST, while other spectral indices and sensor
305 bands contributed to a lesser extent.

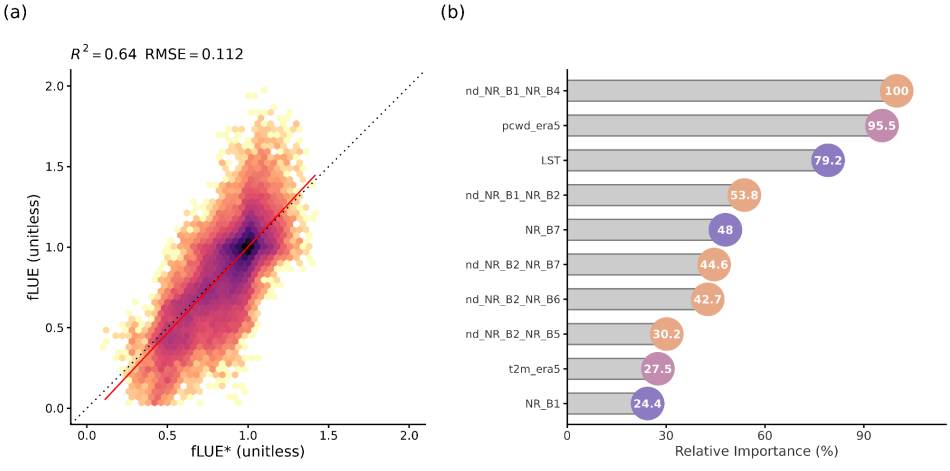

306

307 **Fig. 2.** Regression model performance (a) and variable importance plots (b) for fLUE predictions using
308 MODIS spectral and thermal bands, ERA5-Land variables t2m and ssrd, and potential cumulative water deficit.
309 The prediction performance metrics are quantified on pooled data from predictions for individual held-out sites
310 of each cross-validation folds.

https://doi.org/10.5194/egusphere-2026-5000
Preprint. Discussion started: 1 September 2026

3.2. Comparison of satellite-derived fLUE and vegetation indices

A simple linear correlation analysis between fLUE*, vegetation indices, and fLUE shows that our remote sensing data-based predictions of fLUE (fLUE*) are better correlated to "observed" fLUE than all tested vegetation indices across all clusters (Fig. 3). In the deciduous vegetation cluster (cDD), fLUE* shows the highest median R^2 values (~0.5), followed by vegetation indices NDVI and ARVI (see Table. S1 for a description of all vegetation indices shown here) with median R^2 values around 0.35, but show higher variance across sites, while GRVI had a median R^2 around 0.20. The correlation is stronger in the cDD cluster than in the evergreen cluster (cGR) for all indices tested. In the evergreen cluster, the median is higher for fLUE* than the vegetation indices. However, there is a relatively high variance in performance from site to site. In contrast, very low or no correlations were found between fLUE and these vegetation indices in the cluster with low sensitivity to soil moisture (cLS) (not shown).

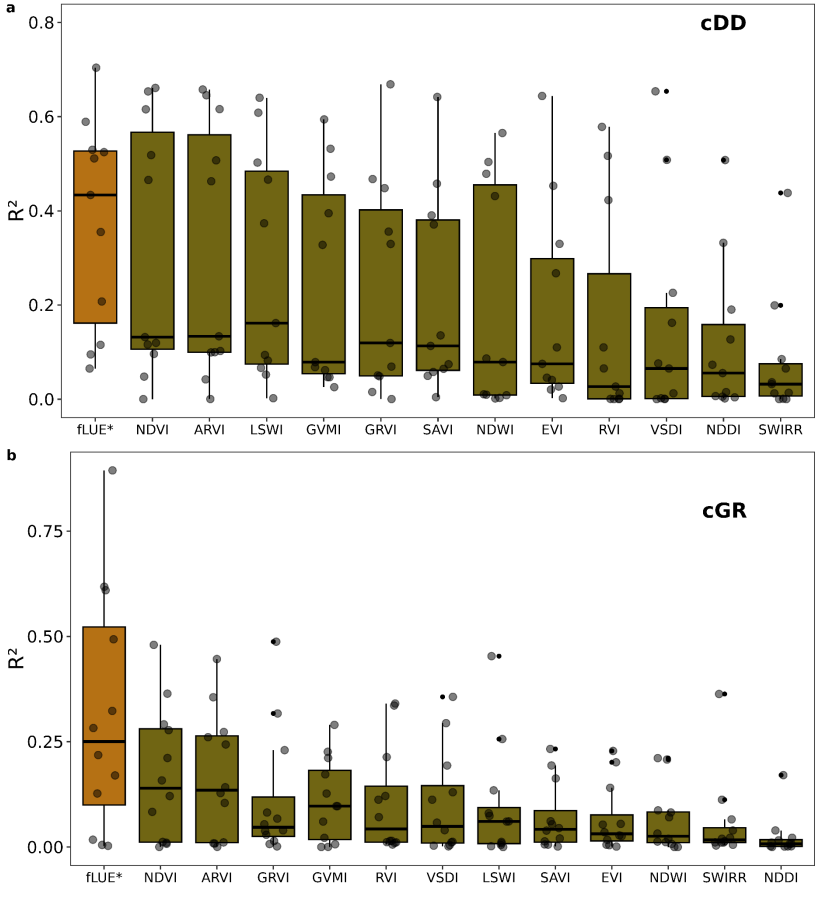

https://doi.org/10.5194/egusphere-2026-5000
Preprint. Discussion started: 1 September 2026

Fig. 3. Linear correlation between fLUE, fLUE*, and selected vegetation indices (Table S1) across the two different clusters of sites (cDD: drought-deciduous cluster and cGR: evergreen cluster). The indices are ranked in decreasing order of the median R^2 for the cGR cluster. Each point indicates the R^2 of fLUE* vs. fLUE for the held-out site from the cross validation for fLUE*.

3.4. Sensing drought responses across Central Europe

Satellite-derived fLUE* and NDVI across central Europe and their evolution over the course of a severe summer drought - from June to August of 2018 - are shown in Fig. 4. For comparison, we also investigated these changes over the course of the relatively moist summer of 2020 (Fig. S2). In general, fLUE* exhibits a stronger decline over summer months than NDVI. In the early drought phase (July), fLUE* records widespread strong reductions (by >0.2 units) across northeastern France, central Germany, and the Netherlands (Fig. 4a), while reductions in NDVI in these regions are much weaker. The magnitudes of both quantities are comparable as they are expressed unitless, between 0 and 1. These differences in early drought phase sensitivity are directly reflected by the map shown in Fig. 5e with a clear dominance of positive values, indicating a stronger decline in fLUE* than in NDVI. The differences in sensitivity between fLUE* and NDVI became even more expressed as the 2018 summer drought progressed (change from June to August, second column in Fig. 4). August-vs.-June reductions of >0.2 fLUE* units are found across most forest regions of northeastern France and central Germany (Fig. 4b). In contrast, reductions appear less pronounced when considering NDVI (Fig. 4d). During the relatively moist summer of 2020, both fLUE* and NDVI increased from June to July in central Germany and the Netherlands compared to the same period in 2018 (Fig. S2a–c). In contrast, fLUE* in northeastern France declined by more than 0.2 units, whereas NDVI exhibited weaker reductions. From June to August, fLUE* again shows a more pronounced decline in August than NDVI (Fig. S2b), with reductions over this period affecting 78% of the study area for fLUE* compared to 60% for NDVI (Fig. S3). As a consequence, we found widespread strong differences between the two metrics across forests of Central Europe, indicating a generally more sensitive response of fLUE* than NDVI.

The Dissimilarity Index threshold derived from the leave-site-out cross-validation structure was 0.195. Of the 3,662,766 valid pixels in the June 2018 prediction raster, 98.29% of the pixels were located inside the model's Area of Applicability, whereas 1.71% were outside. The mean DI was 0.089 ± 0.037, substantially below the applicability threshold, indicating that most spatial predictions were made within predictor conditions represented by the training data. Nevertheless, a small number of pixels showed substantially higher dissimilarity (maximum DI = 1.500), mainly in high altitude areas of the alps (Fig. S4).

https://doi.org/10.5194/egusphere-2026-5000
Preprint. Discussion started: 1 September 2026

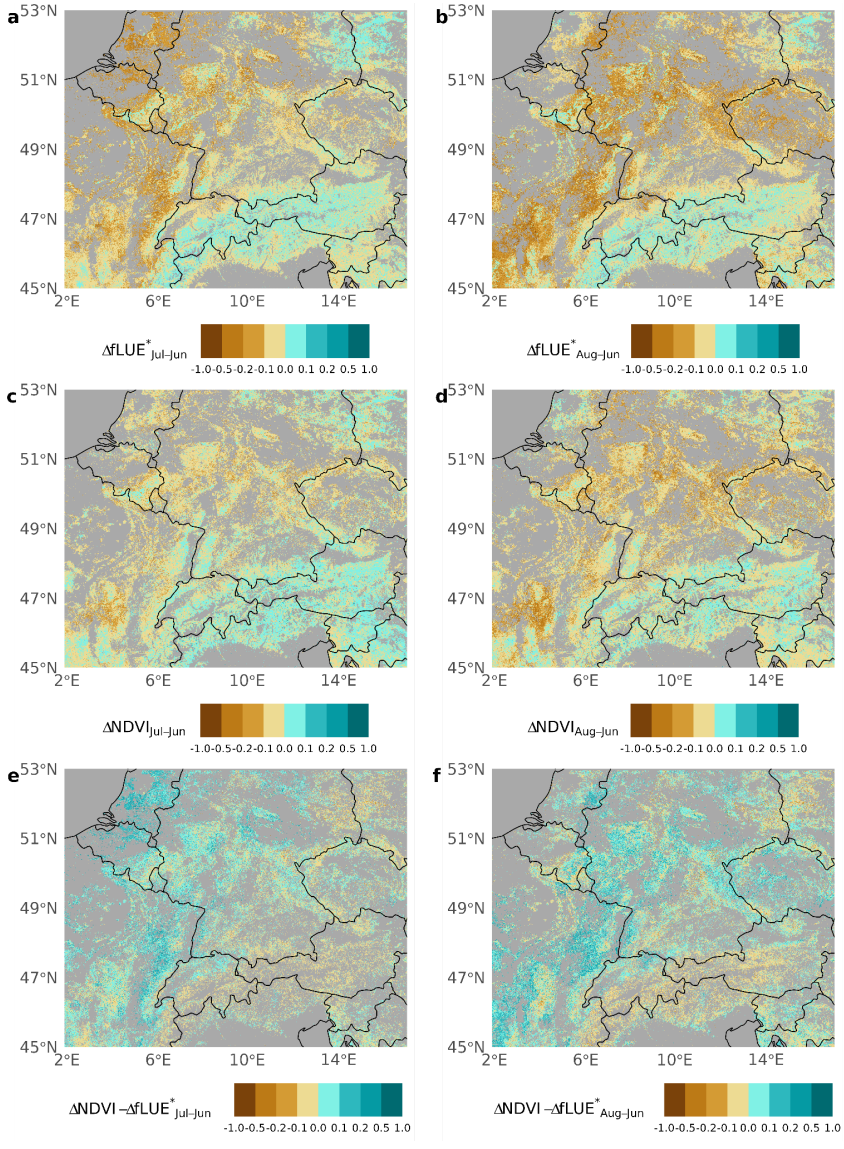

Fig. 4. Spatial patterns of changes in fLUE* and NDVI from June to July (a) and from June to August (b) of 2018. Changes in NDVI for the same periods are shown in (c) and (d), respectively. The difference between temporal changes recorded by NDVI vs. fLUE* for the periods June to July and June to August are shown in (e) and (f), respectively.

https://doi.org/10.5194/egusphere-2026-5000
Preprint. Discussion started: 1 September 2026

3.5. Drought responses across vegetation types

As indicated by our analysis of $fLUE^*$ and NDVI over the course of soil moisture drought at eddy covariance sites (Fig. 3 and Fig. 4), differences in the sensitivity of the two metrics are more expressed in evergreen vegetation. Therefore, we aggregated spatial results shown in Fig. 4 by vegetation type across Central Europe (Fig. 5). This confirms the finding that $fLUE^*$ is much more sensitive than NDVI in evergreen vegetation (strongly positive values for evergreen broadleaf forest, EBF, in Fig. 5c). We also found that this difference is greatest under the relatively moist summer conditions of 2020. $fLUE^*$ generally declined over the course of both summers, considering both the July vs. June and the August vs. June decline, in all vegetation types (except for mixed forests, we found no decline in July vs. June 2020). Interestingly, we also found a strong decline in $fLUE^*$ for 2020 in evergreen broadleaf forests, despite comparably moist conditions in that year. In contrast, NDVI recorded no or only minimal declines for July vs. June 2018 in evergreen vegetation (both broadleaf and needleleaf). For July vs. June 2020, NDVI exhibited an increase or minimal decline for most vegetation types (except grasslands and what was classified as savannah).

https://doi.org/10.5194/egusphere-2026-5000
Preprint. Discussion started: 1 September 2026

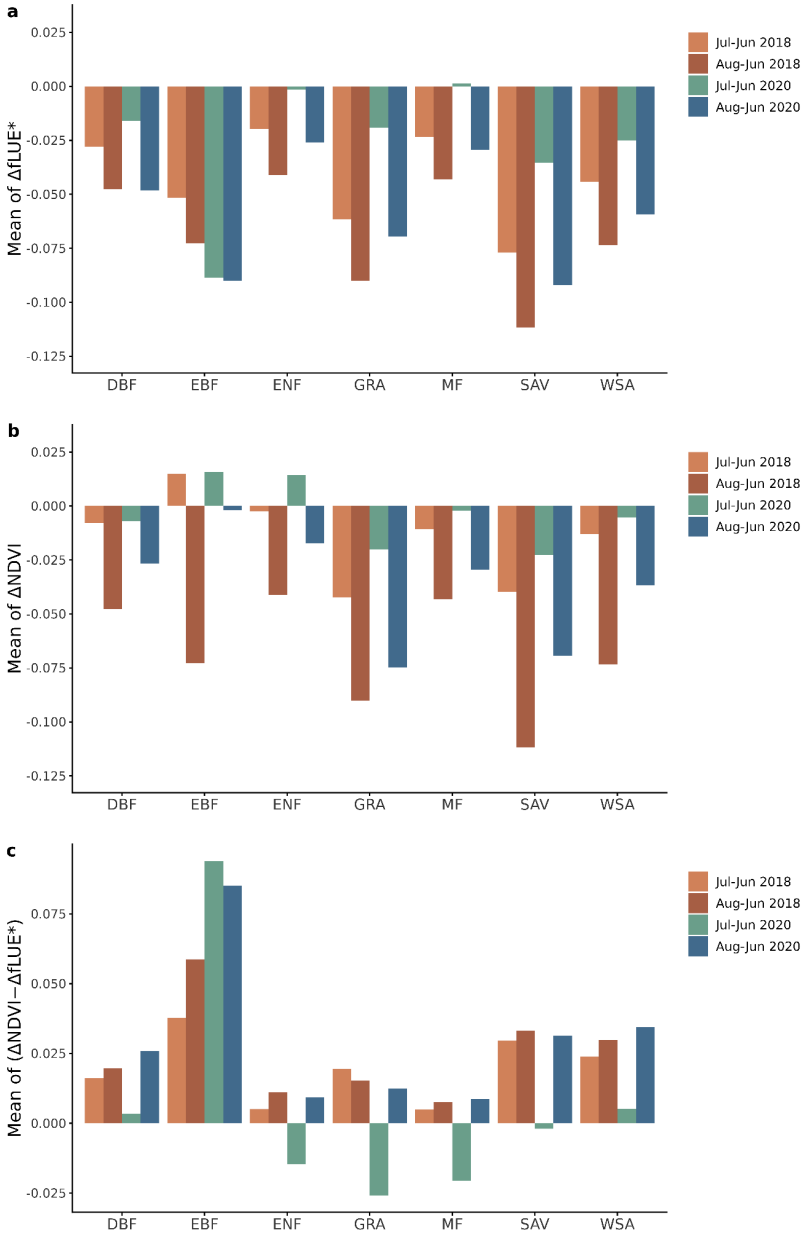

Fig. 5 . Changes in fLUE* (a), NDVI (b), and the difference between the both (c) for each vegetation type during the summers of 2018 and 2020, comparing July vs. June values and August vs. June values. Values are averages over areas covered by each type within the spatial domain shown in Fig. 5 (GRA: grasslands; SAV: savanna; WSA: woody savanna; ENF: evergreen needleleaf forest; EBF: evergreen broadleaf forest; DBF: deciduous broadleaf forest; DNF: deciduous needleleaf forest; MF: mixed forest).

https://doi.org/10.5194/egusphere-2026-5000
Preprint. Discussion started: 1 September 2026

4. Discussion

Greenness-based remote sensing of vegetation could underestimate drought impacts on the carbon cycle due to strong physiological responses of plants to water stress that are not accompanied by simultaneous canopy structural changes (Morton et al. 2014; Hu et al. 2022; B. D. Stocker et al. 2019). Here, we have developed a non-parametric model, informed by multispectral reflectance and thermal remote sensing data, combined with climate reanalysis, for a more accurate quantification of drought impacts on the ecosystem photosynthetic C uptake, focusing on the physiological response. The model was trained on estimates of the soil moisture stress on light use efficiency of photosynthesis, derived from eddy covariance-based ecosystem flux data. The aim was to detect vegetation physiological responses to drought, independent of canopy structural changes, across a wide range of ecosystems.

Greenness indices are widely used for drought impact detection and quantification, but reflect mostly the structural response of ecosystem photosynthesis to drought. A strong effect of water limitation on photosynthesis, independent of declines in greenness, is expected from known mechanisms of the physiological response, including stomatal closure (Martin-StPaul et al. 2017; Abdalla et al. 2021), acclimation of photosynthesis to sustained water stress (Zhou et al. 2013), and the deployment of leaf pigments and NPQ (Müller et al. 2001; Jaume Flexas and Medrano 2002). It remains largely unknown to what extent this component of the drought response can be captured from remote sensing data. While previous studies have targeted the prediction of GPP (Jung et al. 2019), or have evaluated its correlations of GPP with individual vegetation indices (Badgley et al. 2017; John A. Gamon et al. 2016; X. Li et al. 2018), our modeling and analysis targets the non-structural component of the ecosystem photosynthesis response to drought, separated from the structural response captured by vegetation greenness. We investigated (1) how well this non-structural component can be sensed with available satellite remote sensing data, (2) which bands and other modalities provide most information for its sensing, (3) to what extent our index fLUE* improves the estimation of non-structural drought impacts over commonly used vegetation indices, (4) how fLUE* evolved over the course of a recent summer drought in Europe and (5) to what extent its sensitivity differs from NDVI, and (6) how differences vary across vegetation types.

4.1. Spectral, thermal, and meteorological data capture more physiological drought response

Our results show that the physiological response can be partly estimated from multispectral reflectances, land surface temperature sensing, and climate data combined. We found that while the non-structural response is partly correlated with vegetation greenness, as captured by NDVI, the correlation breaks down, particularly in evergreen ecosystems (see also Sec. 4.2), during the early

https://doi.org/10.5194/egusphere-2026-5000
Preprint. Discussion started: 1 September 2026

phases of drought events, and relatively mild water stress conditions. Under these conditions, fLUE* provides a more sensitive metric, reflecting reductions of ecosystem photosynthesis prior to discernible declines in greenness. Under these conditions, our earth observation data-driven model captures a larger portion and an earlier onset of the drought response. This finding rests on multiple results presented here. First, the model demonstrated good performance for spatial generalisation, as measured by the leave-site-out cross-validation performed on a wide variety of sites and vegetation types (R^2 = 0.64, RMSE = 0.112) (Fig. 2a), indicating that it reliably detects vegetation physiological responses to drought across space and diverse vegetation types. The cross-validation setup applied here (leave-site-out) measures the performance of the model estimating water-stress related light use efficiency reductions on a location for which no data was used for model training. This cross-validation setup thus reflects the application of the model here, where it is used for providing water stress effects estimation across space - an essential aspect of reliable model performance assessment (Ludwig et al. 2023; Sweet et al. 2023). Second, the comparison between fLUE* and vegetation indices in capturing physiological effects during drought periods showed that there is a correlation between photosynthetic efficiency and NDVI, but a stronger one when considering the multispectral signal in combination with the thermal signal and meteorological data (as expressed by fLUE*) (Fig. 3). Third, across Central Europe, fLUE* showed earlier, stronger, and more widespread declines starting from July under severe drought conditions of 2018 compared with NDVI in the same regions and periods. Even under the milder drought conditions of 2020, fLUE* declined for many vegetation types (e.g., DBF, EBF, GRA, SAV, and WSA), unlike NDVI. This may partly indicate increasing physiological stress under progressively drier conditions, but it may also reflect seasonal senescence or leaf ageing; disentangling these effects requires further analysis (Fig. 4 and Fig. 5).

Taken together, this shows that there is information in the combination of spectral, thermal, and meteorological data that is untapped by traditional vegetation indices and that can be used for a more complete estimation of drought impacts on vegetation functioning from earth observation data. Our analysis identifies the environmental conditions and vegetation types under which incorporating these data sources alters assessment of drought impacts on vegetation functioning.

Previous studies have shown a close link between photosynthetic efficiency and canopy greenness. Using only NDVI and LST from MODIS, LUE was estimated with an R^2 of 0.73 (Wu and Niu 2012; S. Wang et al. 2017). However, while such vegetation indices can effectively track LUE at broader time scales, they may be less sensitive to short-term environmental stress. Our spatial prediction during drought events reveals this limitation directly in many ecosystems. In contrast, our work estimates LUE reduction in response to soil moisture drought on a sub-seasonal timescale, capturing rapid physiological stress even under mild drought conditions, when structural or pigment-related changes are limited and often missed by greenness-based indices (Fig. 5). Over longer periods, VIs

https://doi.org/10.5194/egusphere-2026-5000
Preprint. Discussion started: 1 September 2026

can still capture stress-related changes in pigment composition, but they often don't respond as directly to rapid changes in photosynthesis efficiency (Rossini et al. 2015) - in particular in locations with evergreen vegetation cover.

Our model does not rely solely on spectral or thermal information but also learns from meteorological drivers of drought, as reflected by the variable importance analysis (Fig. 2b). This integration enables the model to better capture the causal link between atmospheric forcing and physiological response. Our findings show that GRVI exerted a particularly strong influence as a predictor of reduced photosynthetic efficiency (fLUE*) (Fig. 2b–c). This pattern reflects the well-established physiological basis of GRVI as an indicator of pigment dynamics (Yin et al. 2022; Nagai et al. 2012). Specifically, GRVI has been demonstrated to be a robust proxy for the Chlorophyll/Carotenoid Index and directly tracks xanthophyll cycle activity (Yin et al. 2022). The xanthophyll cycle is a key photoprotective mechanism that down-regulates photosynthetic efficiency under stress conditions (Demmig-Adams and Adams 1996). This mechanistic link is further supported by evidence that GRVI correlates more strongly with the forest canopy's maximum photosynthetic capacity than NDVI or EVI, confirming its high sensitivity to the pigment-driven changes that control photosynthetic function (Nagai et al. 2012).

The secondary yet critical roles of PCWD and LST contextualize the primary spectral signal. PCWD reflects the atmospheric drought forcing (Gimeno-Sotelo et al. 2024). This is supported by Buras et al. (2020), who showed at the continental scale that precipitation and temperature anomalies are the second- and third-most critical drivers of early wilting during severe drought in Central Europe. PCWD importance confirms that the reduction in photosynthetic efficiency (fLUE*) is a direct response to cumulative water stress. On the other hand, LST captures effects of water-stress induced stomatal closure and reduced vegetation activity, including transpiration and photosynthesis (Ma et al. 2022; Geng et al. 2023; Mullapudi et al. 2023). The physiological response to water stress is strongly driven by stomatal regulation and changes in photosynthetic capacities (J. Flexas et al. 2004; Zhou et al. 2013). Stomatal regulation reduces water loss through transpiration, but also affects the surface energy partitioning, leading to a heating of transpiring surfaces and leaves, more sensible heat flux, while reducing the latent heat flux. Therefore, LST reflects stomatal regulation and thereby the physiological response (Jiang et al. 2023; Lian et al. 2021; Zhang et al. 2025). These results suggest that the integration of simple spectral indices from the visible range with key meteorological drivers and the thermal infrared-based signal (LST) offers a robust approach for detecting the physiological response of ecosystems during drought more than vegetation indices alone. While expected, given fLUE was used as the training target, this highlights how specific and voluminous training data for targeted machine learning models can yield more reliable and sensitive estimates of drought effects than parametric regression models (indices) can do.

https://doi.org/10.5194/egusphere-2026-5000
Preprint. Discussion started: 1 September 2026

4.2. Clearest advantage in evergreen vegetation

Evergreen forests present a challenge for remotely detecting physiological stress because they show little variation in foliage over the course of the year and hence canopy greenness is often maintained under environmental stress (Hmimina et al. 2013). The spatial prediction of vegetation responses during drought events showed distinct patterns in NDVI and our satellite-derived fLUE (Fig. 4). fLUE* responds to drought earlier than NDVI, showing a stronger reduction in many regions in July, and continuing into August during the severe 2018 drought (Fig. 4e–f) Spatial aggregation by vegetation type across Central Europe showed a consistent fLUE* decline for all vegetation types during the summer droughts of 2018 and 2020, while NDVI failed to capture these changes, especially in evergreen forests, where it decreased only under the severe drought conditions of August 2018 (Fig. 5). A similar, yet nuanced, decoupling is observed in DBF. Here, fLUE* also shows a greater decline than NDVI in both years, with the most severe physiological stress occurring during late summer (August). While a classic remote-sensing symptom of severe drought in DBF is "early wilting" or leaf shedding (a sharp NDVI drop) (Brun et al. 2020), our results show that moderate mid-summer water stress (e.g., in July) is less captured by NDVI. Our fLUE* model, however, reliably detects this early-stage physiological decline, showing a stronger reduction in July than NDVI (Fig. 5). Consistent with previous studies that identified over 30,000 km² of deciduous forest in Central Europe falling within the lowest VI quantile during the 2018 drought (Buras et al., 2020). The substantial NDVI reductions have been associated with early leaf shedding, a mechanism to reduce overall tree transpiration and water loss (Schuldt et al. 2020; Brun et al. 2020; Buras, Rammig, and Zang 2020; Descals et al. 2023). NDVI also increased in some locations during dry periods (Fig. 4c), while fLUE remains around 1.0 under the same conditions. The NDVI increase is likely due to drought-associated sunny conditions under typically energy-limited rather than water-limited site conditions. This can enhance photosynthetic activity and thus vegetation greening (Mastrotheodoros et al. 2020; W. Li et al. 2023).

In contrast, evergreen forests showed only slight variations in NDVI during mid-summer droughts (Fig. 5b) make it challenging to remotely detect drought impacts. These biomes remain green year-round, and visible signs such as leaf shedding or discoloration typically indicate only severe stress or mortality (Huang and Xia 2019; Brun et al. 2020). Our findings reflect this pattern. While EBF and ENF showed minimal or positive NDVI changes in July 2018 and 2020, followed by a sharp decline only under extreme August 2018 stress (likely indicating irreversible damages), our fLUE* metric revealed a consistent and significant physiological downregulation beginning in July for both evergreen types (Fig. 5a–b).

The model was evaluated across a diverse set of sites spanning multiple biomes and continents, indicating that it is broadly applicable across a wide range of ecosystem types. However, its practical

https://doi.org/10.5194/egusphere-2026-5000
Preprint. Discussion started: 1 September 2026

application is demonstrated here only for a temperate European region, so further testing is still needed in other contrasting climatic regimes. The finding that fLUE* is particularly effective at detecting water stress in evergreen vegetation. This suggests considerable potential for application in subtropical and tropical ecosystems characterized by closed evergreen canopies and pronounced seasonal water limitations, including monsoon-influenced regions where timely detection of drought stress remains challenging.

4.3. Opportunities

Several methodological and observational aspects motivated our study. First, fLUE (B. D. Stocker et al. 2018) provided a physiologically meaningful target variable derived from eddy-covariance flux measurements, with a large data volume and broad ecological representativeness across sites, offering a robust empirical basis for model training and evaluation across diverse conditions. Second, readily accessible satellite observations from the MODIS mission provide more than two decades of consistent global coverage. Although the spatial resolution is moderate (500 m), MODIS combines multiple complementary data streams, including visible, near-infrared, and thermal infrared observations at a spatial resolution that matches the typical spatial extent of eddy-covariance measurements' footprints (Chu et al. 2021). Third, readily available machine-learning methods constitute an effective tool for modelling complex, nonlinear relationships and interactions, while enabling robust generalization.

Future Earth observation missions may open new opportunities for using multi-source observations for the accurate detection of physiological drought responses and photosynthetic activity. Upcoming thermal remote sensing missions at high spatial resolution, or optical remote sensing with enhanced spectral resolution and targeted sensing of solar-induced chlorophyll fluorescence (SIF), bear potential for improving flux data-informed models in the future. In contrast, multispectral remote sensing with high spatial resolution is not necessarily advantageous for this purpose, as the characteristic footprint of eddy-covariance towers in forested systems (typically on the order of ~1 km) is inherently well matched to moderate-resolution products such as those from MODIS or VIIRS (Chu et al. 2021). Using higher-resolution imagery is not straightforward, because it requires explicit consideration of sub-footprint heterogeneity. Uncertainties related to spatial and temporal representativeness must thus be addressed to account for temporally varying source areas determined by wind direction (B. Chen et al. 2010).

https://doi.org/10.5194/egusphere-2026-5000
Preprint. Discussion started: 1 September 2026

5. Conclusions

This study demonstrates that a data-driven integration of multispectral reflectance, thermal information, meteorological drivers, and flux-derived target data can retrieve the ecosystem-scale physiological drought responses more effectively than greenness-based vegetation indices alone. By using fLUE as a physiologically meaningful target, measuring the water stress-related reduction in the light use efficiency of photosynthesis, and a machine-learning framework that generalizes across sites, we show that drought impacts on photosynthetic activity can be detected earlier and more sensitively than with NDVI and related indices, especially in evergreen vegetation where structural signals are weak. Our approach demonstrates how current available satellite observations, combined with flux data and machine learning, systematically separates the physiological response from the greenness-related response to soil moisture stress. Our modelling approach is adaptable to integrate future high spatio-temporal resolution products, ensuring continuity and improved investigation of separated vegetation structural and physiological dynamics of vegetation on the global scale.

Code/Data availability

MODIS data are publicly available through NASA's AppEEARS platform: https://appeears.earthdatacloud.nasa.gov/. The fLUE dataset is available on Zenodo: https://zenodo.org/records/1158524. All code used in this study, together with the machine-learning dataset, is available in the GitHub repository : https://github.com/yousra07/index_based_physiological_drought.

Competing interests

The authors declare no conflicts of interest relevant to this study

Author contributions

YEM downloaded and prepared the data for modelling and analysis, conducted the analyses, produced visualisations, interpreted the results, wrote the first draft of the manuscript, and revised the manuscript. BDS and KH designed the study. KH developed the initial MODIS data-processing and modelling framework and reviewed the manuscript. BDS refined the model and data-imputation approach, contributed to the methodology and interpretation, and revised the manuscript.

https://doi.org/10.5194/egusphere-2026-5000
Preprint. Discussion started: 1 September 2026

References

Abdalla, Mohanned, Mutez Ali Ahmed, Gaochao Cai, et al. 2021. "Stomatal Closure during Water Deficit Is Controlled by Below-Ground Hydraulics." *Annals of Botany* 129 (2): 161–70. https://doi.org/10.1093/aob/mcab141.

Badgley, Grayson, Christopher B. Field, and Joseph A. Berry. 2017. "Canopy Near-Infrared Reflectance and Terrestrial Photosynthesis." *Science Advances* 3 (3): e1602244. https://doi.org/10.1126/sciadv.1602244.

Brun, Philipp, Achilleas Psomas, Christian Ginzler, Wilfried Thuiller, Massimiliano Zappa, and Niklaus E. Zimmermann. 2020. "Large-Scale Early-Wilting Response of Central European Forests to the 2018 Extreme Drought." *Global Change Biology* 26 (12): 7021–35. https://doi.org/10.1111/gcb.15360.

Cai, Wenjia, Ziqi Zhu, Sandy P. Harrison, et al. 2025. "A Unifying Principle for Global Greenness Patterns and Trends." *Communications Earth & Environment* 6 (1): 19. https://doi.org/10.1038/s43247-025-01992-0.

Chaudhari, Shilpa, Vandana Sardar, and Prosenjit Ghosh. 2023. "Drought Classification and Prediction with Satellite Image-Based Indices Using Variants of Deep Learning Models." *International Journal of Information Technology* 15 (7): 3463–72. https://doi.org/10.1007/s41870-023-01379-4.

Chen, B., Q. Ge, D. Fu, et al. 2010. "A Data-Model Fusion Approach for Upscaling Gross Ecosystem Productivity to the Landscape Scale Based on Remote Sensing and Flux Footprint Modelling." *Biogeosciences* 7 (9): 2943–58. https://doi.org/10.5194/bg-7-2943-2010.

Chen, Liangzhi, Philipp Brun, Pascal Buri, et al. 2025. "Global Increase in the Occurrence and Impact of Multiyear Droughts." *Science* 387 (6731): 278–84. https://doi.org/10.1126/science.ado4245.

Chu, Housen, Xiangzhong Luo, Zutao Ouyang, et al. 2021. "Representativeness of Eddy-Covariance Flux Footprints for Areas Surrounding AmeriFlux Sites." *Agricultural and Forest Meteorology* 301–302 (May): 108350. https://doi.org/10.1016/j.agrformet.2021.108350.

Cowan, I. R., and G. D. Farquhar. 1977. "Stomatal Function in Relation to Leaf Metabolism and Environment." *Symp. Soc. Exp. Biol.* 31: 471–505.

Davis, Tyler W., I. Colin Prentice, Benjamin D. Stocker, et al. 2017. "Simple Process-Led Algorithms for Simulating Habitats (SPLASH v.1.0): Robust Indices of Radiation, Evapotranspiration and Plant-Available Moisture." *Geoscientific Model Development* 10 (2): 689–708. https://doi.org/10.5194/gmd-10-689-2017.

Demmig-Adams, Barbara, and William W. Adams III. 2006. "Photoprotection in an Ecological Context: The Remarkable Complexity of Thermal Energy Dissipation." *New Phytologist* 172 (1): 11–21. https://doi.org/10.1111/j.1469-8137.2006.01835.x.

Demmig-Adams, Barbara, and William W. Adams. 1996. "The Role of Xanthophyll Cycle Carotenoids in the Protection of Photosynthesis." *Trends in Plant Science* 1 (1): 21–26. https://doi.org/10.1016/S1360-1385(96)80019-7.

D'Odorico, Petra, Leonie Schönbeck, Valentina Vitali, et al. 2021a. "Drone-based Physiological Index Reveals Long-term Acclimation and Drought Stress Responses in Trees." *Plant, Cell & Environment* 44 (11): 3552–70. https://doi.org/10.1111/pce.14177.

D'Odorico, Petra, Leonie Schönbeck, Valentina Vitali, et al. 2021b. "Drone-Based Physiological Index Reveals Long-Term Acclimation and Drought Stress Responses in Trees." *Plant, Cell & Environment* 44 (11): 3552–70. https://doi.org/10.1111/pce.14177.

Flexas, J., J. Bota, F. Loreto, G. Cornic, and T. D. Sharkey. 2004. "Diffusive and Metabolic Limitations to Photosynthesis under Drought and Salinity in C3 Plants." *Plant Biology* 6 (3): 269–79. https://doi.org/10.1055/s-2004-820867.

Flexas, Jaume, and Hipólito Medrano. 2002. "Energy Dissipation in C3 Plants under Drought." *Functional Plant Biology: FPB* 29 (10): 1209–15. https://doi.org/10.1071/FP02015.

Gamon, J. A., J. Peñuelas, and C. B. Field. 1992. "A Narrow-Waveband Spectral Index That Tracks Diurnal Changes in Photosynthetic Efficiency." *Remote Sensing of Environment* 41 (1): 35–44. https://doi.org/10.1016/0034-4257(92)90059-S.

Gamon, John A., K. Fred Huemmrich, Christopher Y. S. Wong, et al. 2016. "A Remotely Sensed

https://doi.org/10.5194/egusphere-2026-5000
Preprint. Discussion started: 1 September 2026

Pigment Index Reveals Photosynthetic Phenology in Evergreen Conifers." *Proceedings of the National Academy of Sciences* 113 (46): 13087–92. https://doi.org/10.1073/pnas.1606162113.

Garbulsky, Martín F., Josep Peñuelas, John Gamon, Yoshio Inoue, and Iolanda Filella. 2011. "The Photochemical Reflectance Index (PRI) and the Remote Sensing of Leaf, Canopy and Ecosystem Radiation Use Efficiencies: A Review and Meta-Analysis." *Remote Sensing of Environment* 115 (2): 281–97. https://doi.org/10.1016/j.rse.2010.08.023.

Geng, Yun-Jing, Pei Leng, and Zhao-Liang Li. 2023. "A Method for Estimating Surface Soil Moisture from Diurnal Land Surface Temperature Observations over Vegetated Regions: A Preliminary Result over an AmeriFlux Site and the REMEDHUS Network." *Journal of Hydrology* 617 (February): 129020. https://doi.org/10.1016/j.jhydrol.2022.129020.

Gimeno-Sotelo, Luis, Rogert Sorí, Raquel Nieto, Sergio M. Vicente-Serrano, and Luis Gimeno. 2024. "Unravelling the Origin of the Atmospheric Moisture Deficit That Leads to Droughts." *Nature Water* 2 (3): 242–53. https://doi.org/10.1038/s44221-023-00192-4.

Gu, Hongfan, Gaofei Yin, Yajie Yang, et al. 2023. "Satellite-Detected Contrasting Responses of Canopy Structure and Leaf Physiology to Drought." *IEEE Journal of Selected Topics in Applied Earth Observations and Remote Sensing* 16: 2427–36. https://doi.org/10.1109/JSTARS.2023.3247422.

Helpap, Patricia, Stefan Brönnimann, Ralf Hand, Jörg Franke, Christoph C. Raible, and Benjamin D. Stocker. 2026. "Are Modern Droughts Unprecedented?" *AGU Advances* 7 (5): e2026AV002536. https://doi.org/10.1029/2026AV002536.

Hermann, Mauro, Matthias Röthlisberger, Arthur Gessler, et al. 2023. "Meteorological History of Low-Forest-Greenness Events in Europe in 2002–2022." *Biogeosciences* 20 (6): 1155–80. https://doi.org/10.5194/bg-20-1155-2023.

Hu, Zhongmin, Shilong Piao, Alan K. Knapp, et al. 2022. "Decoupling of Greenness and Gross Primary Productivity as Aridity Decreases." *Remote Sensing of Environment* 279 (September): 113120. https://doi.org/10.1016/j.rse.2022.113120.

Huang, Kun, and Jianyang Xia. 2019. "High Ecosystem Stability of Evergreen Broadleaf Forests under Severe Droughts." *Global Change Biology* 25 (10): 3494–503. https://doi.org/10.1111/gcb.14748.

Hufkens, Koen, and Benjamin Stocker. 2024. "FluxDataKit v3.3: A Comprehensive Data Set of Ecosystem Fluxes for Land Surface Modelling." Zenodo, July 25. https://doi.org/10.5281/zenodo.12818273.

Jahns, Peter, and Alfred R. Holzwarth. 2012. "The Role of the Xanthophyll Cycle and of Lutein in Photoprotection of Photosystem II." *Biochimica et Biophysica Acta (BBA) - Bioenergetics*, Photosystem II, vol. 1817 (1): 182–93. https://doi.org/10.1016/j.bbabio.2011.04.012.

Jiang, Kang, Zhihua Pan, Feifei Pan, et al. 2023. "Combined Influence of Soil Moisture and Atmospheric Humidity on Land Surface Temperature under Different Climatic Background." *iScience* 26 (6): 106837. https://doi.org/10.1016/j.isci.2023.106837.

Jung, Martin, Sujan Koirala, Ulrich Weber, et al. 2019. "The FLUXCOM Ensemble of Global Land-Atmosphere Energy Fluxes." *Scientific Data* 6 (1): 74. https://doi.org/10.1038/s41597-019-0076-8.

Kowalski, Katja, Akpona Okujeni, Maximilian Brell, and Patrick Hostert. 2022. "Quantifying Drought Effects in Central European Grasslands through Regression-Based Unmixing of Intra-Annual Sentinel-2 Time Series." *Remote Sensing of Environment* 268 (January): 112781. https://doi.org/10.1016/j.rse.2021.112781.

Li, Wantong, Gregory Duveiller, Sebastian Wieneke, et al. 2024. "Regulation of the Global Carbon and Water Cycles through Vegetation Structural and Physiological Dynamics." *Environmental Research Letters* 19 (7): 073008. https://doi.org/10.1088/1748-9326/ad5858.

Li, Wantong, Javier Pacheco-Labrador, Mirco Migliavacca, et al. 2023. "Widespread and Complex Drought Effects on Vegetation Physiology Inferred from Space." *Nature Communications* 14 (1): 4640. https://doi.org/10.1038/s41467-023-40226-9.

Li, Xing, Jingfeng Xiao, Binbin He, et al. 2018. "Solar-Induced Chlorophyll Fluorescence Is Strongly Correlated with Terrestrial Photosynthesis for a Wide Variety of Biomes: First Global Analysis Based on OCO-2 and Flux Tower Observations." *Global Change Biology* 24 (9):

https://doi.org/10.5194/egusphere-2026-5000
Preprint. Discussion started: 1 September 2026

3990–4008. https://doi.org/10.1111/gcb.14297.
Lian, Xu, Shilong Piao, Anping Chen, et al. 2021. "Multifaceted Characteristics of Dryland Aridity Changes in a Warming World." *Nature Reviews Earth & Environment* 2 (4): 232–50. https://doi.org/10.1038/s43017-021-00144-0.
Lin, Yan-Shih, Belinda E. Medlyn, Remko A. Duursma, et al. 2015. "Optimal Stomatal Behaviour around the World." *Nature Climate Change* 5 (5): 5. https://doi.org/10.1038/nclimate2550.
Loaiza, David Montero, actions-user, Emanuel Castanho, Francesco Martinuzzi, Cesar Aybar, and Oto Kaláb. 2024. *Awesome-Spectral-Indices/Awesome-Spectral-Indices: 0.6.0*. Version 0.6.0. Zenodo, released May 16. https://doi.org/10.5281/zenodo.11203806.
Ludwig, Marvin, Alvaro Moreno-Martinez, Norbert Hölzel, Edzer Pebesma, and Hanna Meyer. 2023. "Assessing and Improving the Transferability of Current Global Spatial Prediction Models." *Global Ecology and Biogeography* 32 (3): 356–68. https://doi.org/10.1111/geb.13635.
Ma, Yanfei, Ji Zhou, Shaomin Liu, et al. 2022. "Estimation of Evapotranspiration Using All-Weather Land Surface Temperature and Variational Trends with Warming Temperatures for the River Source Region in Southwest China." *Journal of Hydrology* 613 (October): 128346. https://doi.org/10.1016/j.jhydrol.2022.128346.
Martin-StPaul, Nicolas, Sylvain Delzon, and Hervé Cochard. 2017. "Plant Resistance to Drought Depends on Timely Stomatal Closure." *Ecology Letters* 20 (11): 1437–47. https://doi.org/10.1111/ele.12851.
Mastrotheodoros, Theodoros, Christoforos Pappas, Peter Molnar, et al. 2020. "More Green and Less Blue Water in the Alps during Warmer Summers." *Nature Climate Change* 10 (2): 155–61. https://doi.org/10.1038/s41558-019-0676-5.
Medlyn, Belinda E., Remko A. Duursma, Derek Eamus, et al. 2011. "Reconciling the Optimal and Empirical Approaches to Modelling Stomatal Conductance." *Glob. Chang. Biol.* 17 (6): 2134–44.
Meyer, Hanna, Carles Milà, Marvin Ludwig, et al. 2026. *CAST: "caret" Applications for Spatial-Temporal Models*. Version 1.1.1. Released July 15. https://cran.r-project.org/web/packages/CAST/index.html.
Middleton, E. M., K. F. Huemmrich, D. R. Landis, T. A. Black, A. G. Barr, and J. H. McCaughey. 2016. "Photosynthetic Efficiency of Northern Forest Ecosystems Using a MODIS-Derived Photochemical Reflectance Index (PRI)." *Remote Sensing of Environment* 187 (December): 345–66. https://doi.org/10.1016/j.rse.2016.10.021.
Morton, Douglas C., Jyoteshwar Nagol, Claudia C. Carabajal, et al. 2014. "Amazon Forests Maintain Consistent Canopy Structure and Greenness during the Dry Season." *Nature* 506 (7487): 221–24. https://doi.org/10.1038/nature13006.
Mullapudi, Archana, Amol D. Vibhute, Shankar Mali, and Chandrashekhar H. Patil. 2023. "A Review of Agricultural Drought Assessment with Remote Sensing Data: Methods, Issues, Challenges and Opportunities." *Applied Geomatics* 15 (1): 1–13. https://doi.org/10.1007/s12518-022-00484-6.
Müller, P., X. P. Li, and K. K. Niyogi. 2001. "Non-Photochemical Quenching. A Response to Excess Light Energy." *Plant Physiology* 125 (4): 1558–66. https://doi.org/10.1104/pp.125.4.1558.
Muñoz-Sabater, Joaquín, Emanuel Dutra, Anna Agustí-Panareda, et al. 2021. "ERA5-Land: A State-of-the-Art Global Reanalysis Dataset for Land Applications." *Earth System Science Data* 13 (9): 4349–83. https://doi.org/10.5194/essd-13-4349-2021.
Nagai, Shin, Taku M. Saitoh, Hideki Kobayashi, et al. 2012. "In Situ Examination of the Relationship between Various Vegetation Indices and Canopy Phenology in an Evergreen Coniferous Forest, Japan." *International Journal of Remote Sensing* 33 (19): 6202–14. https://doi.org/10.1080/01431161.2012.682660.
Oren, R., J. S. Sperry, G. G. Katul, et al. 1999. "Survey and Synthesis of Intra- and Interspecific Variation in Stomatal Sensitivity to Vapour Pressure Deficit: Intra- and Interspecific Variation in Stomatal Sensitivity to Vapour Pressure Deficit." *Plant, Cell & Environment* 22 (12): 1515–26. https://doi.org/10.1046/j.1365-3040.1999.00513.x.
Pastorello, Gilberto, Carlo Trotta, Eleonora Canfora, et al. 2020. "The FLUXNET2015 Dataset and the ONEFlux Processing Pipeline for Eddy Covariance Data." *Scientific Data* 7 (1): 225.

https://doi.org/10.5194/egusphere-2026-5000
Preprint. Discussion started: 1 September 2026

https://doi.org/10.1038/s41597-020-0534-3.
Qiu, Ruonan, Ge Han, Xing Li, et al. 2024. “Contrasting Responses of Relationship between Solar-Induced Fluorescence and Gross Primary Production to Drought across Aridity Gradients.” *Remote Sensing of Environment* 302 (March): 113984. https://doi.org/10.1016/j.rse.2023.113984.
Reichstein, Markus, Michael Bahn, Philippe Ciais, et al. 2013. “Climate Extremes and the Carbon Cycle.” *Nature* 500 (7462): 287–95. https://doi.org/10.1038/nature12350.
Rossini, M., L. Nedbal, L. Guanter, et al. 2015. “Red and Far Red Sun-Induced Chlorophyll Fluorescence as a Measure of Plant Photosynthesis.” *Geophysical Research Letters* 42 (6): 1632–39. https://doi.org/10.1002/2014GL062943.
Schaaf, C., and Z. Wang. 2021. “MODIS/Terra+Aqua BRDF/Albedo Nadir BRDF-Adjusted Ref Daily L3 Global - 500m V061.” Earth Science Data Systems, NASA, February 4. https://doi.org/10.5067/MODIS/MCD43A4.061.
Stocker, Benjamin. 2018. “fLUE.” Zenodo, January 24. https://doi.org/10.5281/zenodo.1158524.
Stocker, Benjamin D. n.d. *Geco-Bern/Cwd*. R. Version version 1.0. February 9; GECO, released. Accessed December 4, 2025. https://github.com/geco-bern/cwd.
Stocker, Benjamin D., Shersingh Joseph Tumber-Dávila, Alexandra G. Konings, Martha C. Anderson, Christopher Hain, and Robert B. Jackson. 2023. “Global Patterns of Water Storage in the Rooting Zones of Vegetation.” *Nature Geoscience* 16 (3): 3. https://doi.org/10.1038/s41561-023-01125-2.
Stocker, Benjamin D., Jakob Zscheischler, Trevor F. Keenan, I. Colin Prentice, Josep Peñuelas, and Sonia I. Seneviratne. 2018a. “Quantifying Soil Moisture Impacts on Light Use Efficiency across Biomes.” *New Phytologist* 218 (4): 1430–49. https://doi.org/10.1111/nph.15123.
Stocker, Benjamin D., Jakob Zscheischler, Trevor F. Keenan, I. Colin Prentice, Josep Peñuelas, and Sonia I. Seneviratne. 2018b. “Quantifying Soil Moisture Impacts on Light Use Efficiency across Biomes.” *New Phytologist* 218 (4): 1430–49. https://doi.org/10.1111/nph.15123.
Stocker, Benjamin D., Jakob Zscheischler, Trevor F. Keenan, I. Colin Prentice, Sonia I. Seneviratne, and Josep Peñuelas. 2019. “Drought Impacts on Terrestrial Primary Production Underestimated by Satellite Monitoring.” *Nature Geoscience* 12 (4): 264–70. https://doi.org/10.1038/s41561-019-0318-6.
Sweet, Lily-belle, Christoph Müller, Mohit Anand, and Jakob Zscheischler. 2023. “Cross-Validation Strategy Impacts the Performance and Interpretation of Machine Learning Models.” Artificial Intelligence for the Earth Systems. *Artificial Intelligence for the Earth Systems* 2 (4). https://doi.org/10.1175/AIES-D-23-0026.1.
Wan, Z., S. Hook, and G. Hulley. 2021. “MODIS/Terra Land Surface Temperature/Emissivity Daily L3 Global 1km SIN Grid V061 | NASA Earthdata.” Earth Science Data Systems, NASA. https://www.earthdata.nasa.gov/data/catalog/lpcloud-mod11a1-061.
Wang, Siheng, Lifu Zhang, Changping Huang, and Na Qiao. 2017. “An NDVI-Based Vegetation Phenology Is Improved to Be More Consistent with Photosynthesis Dynamics through Applying a Light Use Efficiency Model over Boreal High-Latitude Forests.” *Remote Sensing* 9 (7): 7. https://doi.org/10.3390/rs9070695.
Wang, Yanbing, Cuihai You, Yanhong Gao, et al. 2023. “Seasonal Variations and Drivers of Energy Fluxes and Partitioning along an Aridity Gradient in Temperate Grasslands of Northern China.” *Agricultural and Forest Meteorology* 342 (November): 109736. https://doi.org/10.1016/j.agrformet.2023.109736.
Wang, Ying, Yanan Chen, Jianguang Wen, et al. 2024. “Early Warning of Drought-Induced Vegetation Stress Using Multiple Satellite-Based Ecological Indicators.” *Ecological Indicators* 169 (December): 112857. https://doi.org/10.1016/j.ecolind.2024.112857.
World Meteorol. Organ. (World Meteorological Organization). 2024. “Fraction of Absorbed Photosynthetically Active Radiation (FAPAR).” November 14. https://gcos.wmo.int/site/global-climate-observing-system-gcos/essential-climate-variables/fraction-of-absorbed-photosynthetically-active-radiation-fapar.
Wright, Marvin N., Stefan Wager, and Philipp Probst. 2024. *Ranger: A Fast Implementation of Random Forests*. Version 0.17.0. Released November 8.

https://doi.org/10.5194/egusphere-2026-5000
Preprint. Discussion started: 1 September 2026

https://cran.r-project.org/web/packages/ranger/index.html.

Wu, Chaoyang, and Zheng Niu. 2012. "Modelling Light Use Efficiency Using Vegetation Index and Land Surface Temperature from MODIS in Harvard Forest." *International Journal of Remote Sensing* 33 (7): 2261–76. https://doi.org/10.1080/01431161.2011.608090.

Xie, Fei, and Hui Fan. 2021. "Deriving Drought Indices from MODIS Vegetation Indices (NDVI/EVI) and Land Surface Temperature (LST): Is Data Reconstruction Necessary?" *International Journal of Applied Earth Observation and Geoinformation* 101 (September): 102352. https://doi.org/10.1016/j.jag.2021.102352.

Yin, Gaofei, Aleixandre Verger, Adrià Descals, Iolanda Filella, and Josep Peñuelas. 2022. "A Broadband Green-Red Vegetation Index for Monitoring Gross Primary Production Phenology." *Journal of Remote Sensing* 2022 (March). https://doi.org/10.34133/2022/9764982.

Zhang, Ziyuan, Xiao Chen, Kang Jiang, et al. 2025. "Dynamics and Interactions of Soil Moisture and Temperature in Semi-Arid Regions of Northern China." *Journal of Arid Environments* 227 (March): 105327. https://doi.org/10.1016/j.jaridenv.2025.105327.

Zhou, Shuangxi, Remko A. Duursma, Belinda E. Medlyn, Jeff W. G. Kelly, and I. Colin Prentice. 2013. "How Should We Model Plant Responses to Drought? An Analysis of Stomatal and Non-Stomatal Responses to Water Stress." *Agricultural and Forest Meteorology* 182–183 (December): 204–14. https://doi.org/10.1016/j.agrformet.2013.05.009.

Zscheischler, Jakob, Miguel D. Mahecha, Stefan Harmeling, and Markus Reichstein. 2013. "Detection and Attribution of Large Spatiotemporal Extreme Events in Earth Observation Data." *Ecological Informatics* 15 (May): 66–73. https://doi.org/10.1016/j.ecoinf.2013.03.004.